Fermilab FERMILAB-Conf-01/090-E D0 July 2001

RECENT QCD RESULTS FROM DØ AT THE TEVATRON

E. J. GALLAS
FOR THE DØ COLLABORATION
Fermi National Accelerator Laboratory, Batavia, Illinois 60510, USA
E-mail: eggs@fnal.gov

The DØ experiment at the Tevatron proton-antiproton collider accumulated a large sample of high energy jet production data during Run I (1992-1996). Presented here are measurements of the inclusive jet cross section at a center-of-mass energy $\sqrt{s} = 1800$ GeV, and a ratio of central inclusive jet cross sections at two different center-of-mass energies (1800 and 630 GeV). Also included is a measure of the ratio of multijet production cross sections at the higher $\sqrt{s}$. All measurements are compared to next-to-leading order QCD predictions with recent parton distribution functions (PDFs). Due to decreased statistical and systematic errors in the measurement, comparison with the theory shows that the prediction may benefit from an increased order in the calculation and from inclusion of proton-antiproton jet data in new global PDF fits.

1 Introduction

The Tevatron collider program completed its first run of data taking in early 1996. The large sample collected by the DØ experiment enables a number of jet measurements which can be compared to predictions from Standard Model QCD. Measurements included in this presentation are:

- the inclusive jet cross section at a proton-antiproton center-of-mass energy $\sqrt{s} = 1800$ GeV, extending previous measurements into the forward region of pseudorapidity ($|\eta| < 3.0$)
- the ratio of this cross section to that at a lower energy ($\sqrt{s} = 630 GeV$) in the central region of pseudorapidity ($|\eta| < 0.5$)
- the ratio of inclusive three-jet to inclusive two-jet production cross sections (R_{32}) at the higher $\sqrt{s} = 1800$ GeV

These measurements are compared to next-to-leading order (NLO) QCD predictions of JETRAD [1] using a number of recent parton distribution functions [2,3,4]. Further details of these results may be found in the References [5,6,7].

2 The Event Samples

All jet measurements described here use primarily calorimetry to identify jets and measure their energy and orientation. Jets are reconstructed using an iterative algorithm with a fixed cone size of radius $R = 0.7$ in $\eta - \phi$ space.

The pseudorapidity is defined as $\eta = -\ln[\tan\frac{\theta}{2}]$, where θ is the angle of the jet relative to the incoming proton beam. The angle ϕ is the azimuthal angle about the beam axis. Vertex, jet and event quality criteria reduce backgrounds caused by electrons, photons, noise and cosmic rays. Additional corrections are applied to obtain jet energies corrected for calorimeter response, noise, showering outside of the cone radius, and energy deposits from spectator interactions. For the inclusive cross sections, unsmearing corrections are applied to remove the effect of a finite jet energy resolution.

The measurements of inclusive cross section at the higher energy ($\sqrt{s} = 1800$ GeV) used an integrated luminosity of nearly 100 pb^{-1} of data. An integrated luminosity of 537 nb^{-1} was available for the inclusive cross section at the lower energy ($\sqrt{s} = 630$ GeV). About 10 pb^{-1} was selected to measure the multijet ratio to reduce systematic uncertainties in the energy scale at higher luminosities. Details of the jet finding algorithm, jet reconstruction, event selection, and measurements can be found through the References [5,6,7].

Jets are the manifestation of partons produced in the primary parton-parton collision. Partons in the NLO calculation may have any angular separation, while the cone of fixed size used to experimentally reconstruct jets may envelop more than one NLO parton. Therefore, partons in the NLO calculations are required to be separated by an angular difference of $\Delta R_{sep} = 1.3 \times R$ in order to be counted as distinct jets.

A χ^2 statistic including both statistical and systematic uncertainties in the theory and data is used in all cases to quantitatively assess the agreement of the predictions with the measurements.

3 Inclusive Jet Cross Section

Data recorded by the DØ detector in Run I yields a high statistics measurement of the inclusive jet cross section over a wide range in jet transverse energy (E_T), where the cross section spans seven orders of magnitude (Figure 1). This new measurement represents the lowest systematic uncertainties to date and includes new data reaching far into the forward regions of pseudorapidity.

An increased cross section at high jet E_T could indicate quark compositeness and/or new physics beyond the Standard Model. Comparison of these cross sections to QCD predictions indicates how well we understand the proton structure: the adequacy of NLO predictions and sensitivity of the predictions to current PDF's (parton distribution functions).

A χ^2 comparison of the measurements to the theory shows that the theory is consistent with the measurements for many of the modern PDF parame-

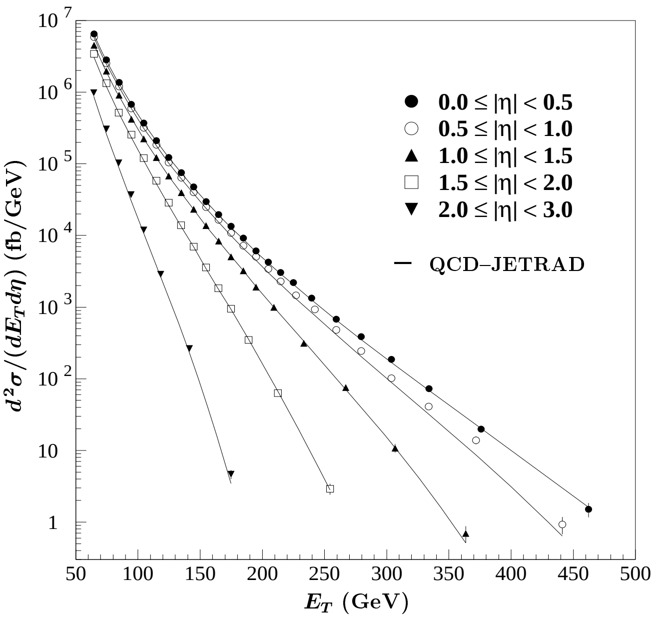

Figure 1. The single inclusive jet production cross section as a function of jet E_T, in five pseudorapidity intervals, showing only statistical uncertainties, along with theoretical predictions.

terizations, such as CTEQ4M and MRSTgU, but finds other PDF's such as CTEQ3M, MRST, and MRSTgD unlikely. A good agreement is seen with the newer CTEQ4HJ PDF, which was contrived using high E_T jet Tevatron collider data, suggesting that the theory should incorporate a higher gluon content at high x than previous PDF's have included. The new jet data is being incorporated in global PDF fits by MRST and CTEQ groups.

4 Ratio of Cross Sections

DØ also recorded data at a center-of-mass energy of 630 GeV during Run I. A dimensionless ratio provides a more stringent test of NLO QCD because of the substantial reduction in both experimental and theoretical uncertainties when taking a ratio. More specifically, we measure the ratio of $R = \sigma_s^{630}/\sigma_s^{1800}$ as a function of x_T, where σ_s is the scale invariant cross section: $\sigma_s = (E_T^3/2\pi)(d^2\sigma/dE_T d\eta)$ and x_T is the jet transverse momentum fraction: $x_T = 2E_T/\sqrt{s}$.

Shown in Figure 2 is the ratio of dimensionless cross sections, R, compared to NLO QCD as given by JETRAD. In the naive parton model, this ratio is flat

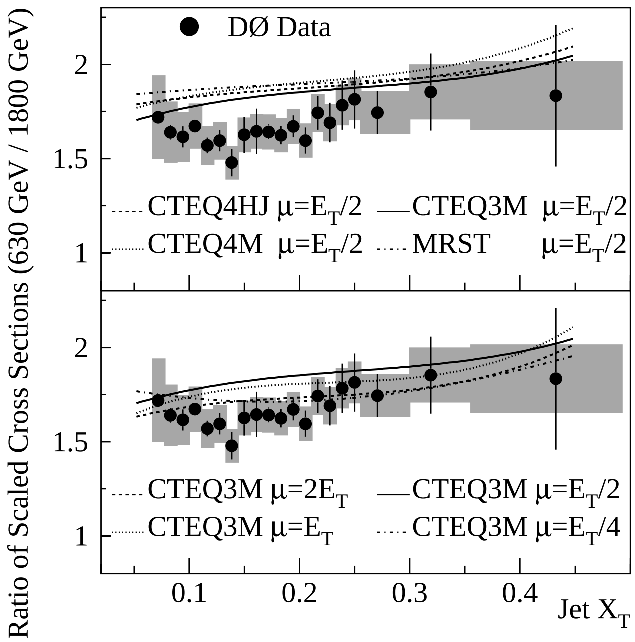

Figure 2. Ratio of dimensionless cross sections (numerator $\sqrt{s}$ = 630 GeV, denominator $\sqrt{s}$ = 1800 GeV) compared to NLO QCD as given by JETRAD.

in x_T. Deviations from this model result from scaling evolution (of both PDF's and α_s) and terms beyond LO. It is interesting to note that as predicted by the theory and verified by experiment, the ratio is greater than 1, expressing that the probability of jet emission is higher for the lower center-of-mass energy at the same x_T (intuitively, emission of lower E_T jets is more likely).

In the χ^2 comparison, NLO predictions for the ratio exhibit satisfactory agreement with the shape of the observed ratio. The choice of PDF has little effect on the result. In terms of only the normalization however, the absolute values of the predictions lie significantly higher than the data, especially for the standard scale ($\mu_R = E_T^{max}/2$). To summarize, further corrections to the NLO calculation seem to be required to reduce the scale dependence and improve the predictive power of the calculation.

5 R_{32}

The ratio of inclusive three-jet to inclusive two-jet production reflects the rate of gluon emission in QCD jet production processes. A three jet cross section explicitly offers the opportunity to investigate scale differences at a secondary vertex (a subsequent gluon emission). Taking the ratio reduces systematic uncertainties.

We measure the ratio

$$R_{32} = \frac{\sigma_3}{\sigma_2} = \frac{\sigma(p\overline{p} \to n \text{ jets} + X; n \geq 3)}{\sigma(p\overline{p} \to m \text{ jets} + X; m \geq 2)}$$

as a function of the scalar sum of jet transverse energies ($H_T = \sum E_T^{\text{jet}}$). The measurement is performed with four distinct sets of selection criteria for all jets in the event: E_T thresholds of $20, 30$, or 40 GeV for $|\eta_{\text{jet}}| < 3$, and $E_T > 20$ GeV for $|\eta_{\text{jet}}| < 2$. Three thresholds were chosen to study threshold dependence, and the minimum threshold was chosen to maximize statistics for which jet reconstruction efficiency was nearly 100%. For each threshold, the ratio R_{32} (or roughly the gluon emission rate) rises rapidly below $H_T =$ 200 GeV and levels off to about $70\%, 60\%$ and 50% as the minimum jet E_T threshold rises from 20 to 30 to 40 GeV, respectively ($|\eta_{\text{jet}}| < 3$).

To study the effect of a different μ_R scale on the production of additional jets, the renormalization scale of the third jet is varied from $\mu_R^{(3)} = \lambda H_T$ (same as for the leading jets) to a scale proportional to the E_T of the third jet $\mu_R^{(3)} \propto E_T^{(3)}$. Also, a scale proportional to the maximum jet transverse energy ($E_T^{\max}$) is studied, as this is the usual form used for comparisons of JETRAD to measured jet cross sections.

Figure 3 shows the measured R_{32} as a function of H_T for jet $E_T > 20$ GeV and $|\eta_{\text{jet}}| < 2$. The 20 GeV threshold has good sensitivity to scale in the JETRAD prediction and has reduced statistical uncertainty. The central rapidity region ($|\eta_{\text{jet}}| < 2$) has the best understood jet energy uncertainties and correlations. Although some of the predictions do not visually overlap with the data, acceptable agreement is found for some scales because of the strong point-to-point correlations of the data uncertainties which are taken into account in the χ^2 comparison of the various predictions to the data.

Generalizing for all criteria: The scale prescriptions using a softer scale for lower E_T jets did not provide a good fit to the data for any value of λ. The λ independent scale $\mu_R = 0.6 E_T^{\max}$ for all jets yielded good agreement with measurement (probability $p > 57\%$) for the $E_T > 20$ GeV criteria, but the χ^2 rises (and the corresponding probabilities decrease) for the higher E_T thresholds (not shown). The JETRAD prediction assuming a scale $\mu_R = \lambda H_T$

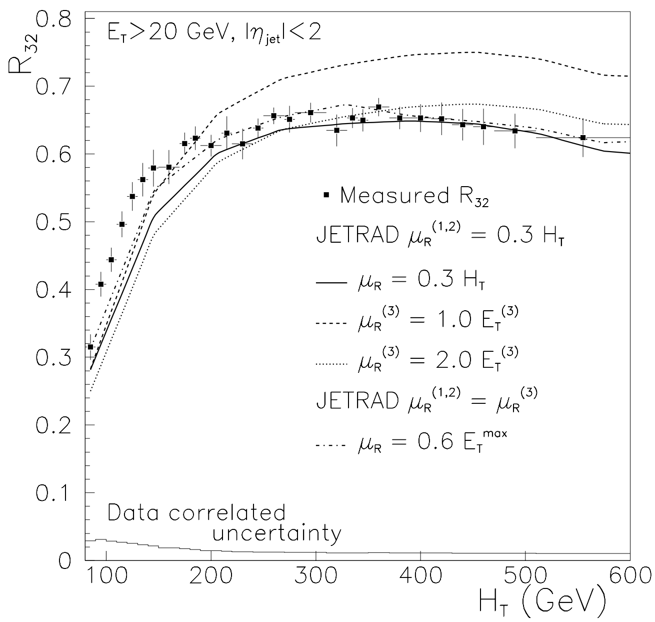

Figure 3. The ratio R_{32} as a function of H_T, requiring jet $E_T > 20$ GeV and $|\eta_{\mathrm{jet}}| < 2$. Error bars indicate statistical and uncorrelated systematic uncertainties, while the histogram at the bottom shows the correlated systematic uncertainty. The four smoothed distributions show the JETRAD prediction for the renormalization scales indicated in the legend.

provides the best description of the data for λ between 0.30 and 0.35 ($p >$ 80%). Moreover, the χ^2 is also minimized in the $\lambda \approx 0.30$ region for the other selection criteria (not shown) making this scale choice the most robust of all the μ_R scales studied.

Although a few scale prescriptions did provide predictions which yielded good fits to this particular measurement, the applicability of those scales in predicting other jet production characteristics is unclear. Reduced scale dependence would improve the predictive power of the theory.

6 Conclusions

It is interesting to note that for Run I jets, overall uncertainties in the measurement are now less than the theoretical uncertainties. In Run II analysis and future calculations, it is therefore important to consider in more detail how comparisons can be improved. In particular, DØ is studying the use of new jet reconstruction algorithms (which are more readily compared to theory) and refining techniques for the further reduction of systematic uncertainties in the analysis of the incoming data of Tevatron Run II. We look forward to improved predictions coordinated with these improved techniques to facilitate a deeper understanding of the data/theory comparisons.

Acknowledgments

We thank David Summers, Dieter Zeppenfeld, and Walter Giele for stimulating and helpful discussions. We thank the staffs at Fermilab and collaborating institutions, and acknowledge support from the Department of Energy and National Science Foundation (USA), Commissariat à L'Energie Atomique and CNRS/Institut National de Physique Nucléaire et de Physique des Particules (France), Ministry for Science and Technology and Ministry for Atomic Energy (Russia), CAPES and CNPq (Brazil), Departments of Atomic Energy and Science and Education (India), Colciencias (Colombia), CONACyT (Mexico), Ministry of Education and KOSEF (Korea), CONICET and UBACyT (Argentina), The Foundation for Fundamental Research on Matter (The Netherlands), PPARC (United Kingdom), Ministry of Education (Czech Republic), and the A.P. Sloan Foundation.

References

1. W.T. Giele, E.W.N. Glover, David A. Kosower, *Nucl. Phys.* B **403**, 633 (1993).
2. H.L. Lai *et al.*, *Phys. Rev.* D **51**, 4763 (1995).
3. A.D. Martin *et al.*, *Eur. Phys. J.* C **4**, 463 (1998).
4. H.L. Lai *et al.*, *Phys. Rev.* D **55**, 1280 (1997).
5. B. Abbott *et al*, *Phys. Rev. Lett.* **86**, 1707 (2001).
6. B. Abbott *et al*, *Phys. Rev. Lett.* **86**, 2523 (2001).
7. B. Abbott *et al*, *Phys. Rev. Lett.* **86**, 1955 (2001).